Organization of cardiac chamber progenitors in the zebrafish blastula

Brian R. Keegan[1], Dirk Meyer[2] and Deborah Yelon[1,*]

[1]Developmental Genetics Program and Department of Cell Biology, Skirball Institute of Biomolecular Medicine, New York University School of Medicine, New York, NY 10016, USA
[2]Department of Developmental Biology, Biology I, University of Freiburg, Freiburg, Germany
*Author for correspondence (e-mail: yelon@saturn.med.nyu.edu)

Accepted 22 March 2004

Development 131, 3081-3091
Published by The Company of Biologists 2004
doi:10.1242/dev.01185

Summary

Organogenesis requires the specification of a variety of cell types and the organization of these cells into a particular three-dimensional configuration. The embryonic vertebrate heart is organized into two major chambers, the ventricle and atrium, each consisting of two tissue layers, the myocardium and endocardium. The cellular and molecular mechanisms responsible for the separation of ventricular and atrial lineages are not well understood. To test models of cardiac chamber specification, we generated a high-resolution fate map of cardiac chamber progenitors in the zebrafish embryo at 40% epiboly, a stage prior to the initiation of gastrulation. Our map reveals a distinct spatial organization of myocardial progenitors: ventricular myocardial progenitors are positioned closer to the margin and to the dorsal midline than are atrial myocardial progenitors. By contrast, ventricular and atrial endocardial progenitors are not spatially organized at this stage. The relative orientations of ventricular and atrial myocardial progenitors before and after gastrulation suggest orderly movements of these populations. Furthermore, the initial positions of myocardial progenitors at 40% epiboly indicate that signals residing at the embryonic margin could influence chamber fate assignment. Indeed, via fate mapping, we demonstrate that Nodal signaling promotes ventricular fate specification near the margin, thereby playing an important early role during myocardial patterning.

Movie available online

Key words: Zebrafish, Ventricle, Atrium, Myocardium, Endocardium, Fate map, Nodal

Introduction

In all vertebrates, the embryonic heart is initially partitioned into two major chambers, a ventricle and an atrium, each exhibiting specific morphological and physiological characteristics (Moorman and Christoffels, 2003; Yelon and Stainier, 1999). Furthermore, a number of gene expression differences distinguish the ventricle and the atrium, including genes encoding chamber-specific myosin heavy chains [e.g. *vmhc* and *amhc* in zebrafish ventricular and atrial myocardium, respectively (Yelon et al., 1999; Berdougo et al., 2003)], chamber-specific transcription factors [e.g. *Irx4* in chick and mouse ventricular myocardium (Bao et al., 1999; Bruneau et al., 2000)] and differentially expressed growth factors [e.g. neuregulin expressed at higher levels in mouse ventricular endocardium (Meyer and Birchmeier, 1995)]. Although the structural and functional differences between the cardiac chambers are evident, the mechanisms that establish ventricular and atrial identities are not yet understood.

Prior to heart tube formation, distinct populations of ventricular and atrial myocardial precursors reside within the lateral plate mesoderm (LPM). In chick, LPM fate maps indicate a rostrocaudal organization of ventricular and atrial precursors (DeHaan, 1963; DeHaan, 1965; Hochgreb et al., 2003; Redkar et al., 2001; Stalsberg and DeHaan, 1969), concurring with the regionalized expression patterns of chamber-specific genes (Bisaha and Bader, 1991; Yutzey et al., 1994). Similarly, in zebrafish and mouse, restricted gene expression patterns suggest spatial organization of chamber precursors within the LPM (Yelon et al., 1999; Berdougo et al., 2003; O'Brien et al., 1993; Lyons et al., 1995). Thus, there exists a clear ventricular-atrial pattern within the LPM, but how is this pattern established? Fate maps of the chick embryo suggest that organization of ventricular and atrial lineages begins at early stages, with ventricular progenitors tending to be located in rostral regions of the cardiogenic portion of the primitive streak and atrial progenitors tending to be located more caudally (Garcia-Martinez and Schoenwolf, 1993; Rosenquist, 1970). However, it is not known whether these positional tendencies correlate with a distribution of chamber specification signals within the primitive streak.

In zebrafish, previous lineage analysis has shown that labeling of a single cardiogenic blastomere at the midblastula (2000 cell/high) stage results in labeled progeny in either the ventricle or the atrium, but never in both chambers (Stainier et al., 1993). These data indicate an early separation of ventricular and atrial lineages, but they do not reveal how this separation is regulated. One possibility is that ventricular and atrial progenitors are spatially organized at early stages and are

thereby differentially exposed to key specification signals. Alternatively, ventricular and atrial progenitors could be intermingled within the blastula, with lineage separation mediated by stochastic and/or lateral inhibition mechanisms.

To distinguish between these models of chamber specification, we have constructed a fate map of chamber progenitors in the zebrafish blastula, including analysis of myocardial and endocardial fates in both the ventricle and the atrium. The resolution of our fate map demonstrates that ventricular and atrial myocardial progenitors are spatially organized prior to gastrulation, such that ventricular progenitors are found closer to the embryonic margin and the dorsal midline than are atrial progenitors. By contrast, ventricular and atrial endocardial progenitors are intermixed at this stage. The relative proximity of ventricular myocardial progenitors to the embryonic margin indicates that Nodal signals, which emanate from the margin, could influence ventricular fate assignment. Consistent with this hypothesis, we find that antagonism of Nodal signaling alters the myocardial fate map, demonstrating an important role of the Nodal pathway during cardiac chamber specification.

Materials and methods

Labeling blastomeres at 40% epiboly

Our fate-mapping strategy was a modification of previously described protocols using caged fluorescein as a lineage tracer in zebrafish embryos (Carmany-Rampey and Schier, 2001; Feldman et al., 2000; Gritsman et al., 2000; Kozlowski et al., 1997). We generated embryos by mating adult fish carrying the *Tg(gsc:gfp)* transgene (Doitsidou et al., 2002), and we determined embryonic stages according to a standard staging series (Kimmel et al., 1995). At the one- to two-cell stage, we injected embryos with 0.3 nl of a 2.5% solution of DMNB-caged, biotinylated, lysine-fixable fluorescein dextran (Molecular Probes) dissolved in 5 mg/ml phenol red in 0.2 M KCl. Embryos were maintained in low light or darkness at 28°C, except during labeling, when they were kept at 20°C.

At 40% epiboly [~5 hours post fertilization (hpf)], we oriented embryos laterally in 3% methylcellulose, using the expression of *Tg(gsc:gfp)* to indicate the location of the dorsal margin (Doitsidou et al., 2002). To activate caged fluorescein in individual blastomeres, we exposed cells to a 10 second pulse from a 375 nm pulsed nitrogen laser (MicroPoint Laser System, Photonic Instruments) focused through a 40× water-immersion objective on a Zeiss Axioplan 2 microscope, equipped with a cooled CCD camera (Pentamax, Princeton Instruments) and automated shutters (Uniblitz) controlled by the Metamorph 4.5 Imaging System (Universal Imaging). In each experiment, we labeled a specific number of neighboring blastomeres within a single tier of the deep cell layer (DEL) of the blastoderm. At 40% epiboly, the first four tiers of the DEL are one to three cells thick (Warga and Kimmel, 1990). For consistency between experiments, we always labeled cells in the most superficial layer of the DEL. In several control experiments, we fixed embryos immediately after initial photography (see below) and proceeded with detection of activated fluorescein (see below); results confirmed that labeling was restricted to the intended blastomeres (data not shown).

Recording the location of labeled blastomeres

For each experiment, we recorded the latitude (distance from the margin) and longitude (distance from the dorsal midline) of the labeled blastomeres. Immediately after fluorescein activation, we captured DIC and fluorescent images to record the latitude of the labeled cells; this position is expressed in tiers, or cell diameters, from the margin, with tier 1 being the row of blastomeres closest to the yolk (Fig. 1A-C). Before documenting the longitude of the labeled cells, we incubated embryos for an hour at 20°C, allowing expression of *Tg(gsc:gfp)* to become appropriately robust. We then recorded longitude using animal views; this position is expressed in degrees around the circumference of the embryo, with the center of *Tg(gsc:gfp)* expression defined as 0° (Fig. 1D). To estimate the change in position introduced by waiting 1 hour to record longitude, we compared longitude positions immediately following labeling and 1 hour after labeling. Convergence of labeled blastomeres toward dorsal was always less than 5° (n=13; data not shown).

Fluorescein detection

After labeling, we incubated embryos in the dark until fixation (4% paraformaldehyde in PBS, 4°C overnight). To maximize sensitivity of detection, we used anti-fluorescein immunohistochemistry to identify cells containing activated fluorescein. Following overnight methanol dehydration, we gradually rehydrated embryos with PBS containing 0.1% Tween 20 (PBT). Embryos fixed at 44 hpf were treated with 10 μg/ml proteinase K (Sigma) for 25 minutes. Heat treatment of embryos at 65°C for 10 minutes inactivated endogenous alkaline phosphatase activity. After blocking (5% sheep serum and 2 mg/ml BSA in PBT for 2 hours), we incubated embryos overnight at 4°C with a preadsorbed anti-fluorescein Fab fragment conjugated to alkaline phosphatase (diluted 1:5000; Boehringer Mannheim). After a series of washes (eight washes, 15 minutes each, with 2 mg/ml BSA in PBT), we equilibrated embryos in NTMT (0.1 M Tris-HCL pH 9.5, 50 mM $MgCl_2$, 0.1 M NaCl, 0.1% Tween 20) and stained with the alkaline phosphatase substrates NBT and BCIP (337.5 μg/ml and 175 μg/ml, respectively), generating a blue precipitate.

Counterstaining techniques enhanced visualization of the heart. In some cases, we used the MF20 anti-myosin heavy chain monoclonal antibody (Bader et al., 1982) to recognize myocardium. We incubated embryos with a 1:10 dilution of MF20 hybridoma supernatant overnight at 4°C, followed by detection with a goat anti-mouse Ig(H+L) secondary antibody conjugated to β-galactosidase (1:100 dilution, 2 hours at room temperature; Southern Biotechnology Associates). After washing (four washes, 15 minutes each), we equilibrated embryos in staining buffer (2 mM $MgCl_2$, 0.2% NP-40, 1 mM deoxycholic acid, 5 mM $K_3Fe(CN)_6$, 5 mM $K_4Fe(CN)_6$) and stained with the β-galactosidase substrate 6-Chloro-3-Indoxy-beta-D-galactopyranoside (‘salmon-gal’, 0.5 mg/ml; Biosynth B-7200), generating a pink precipitate (Fig. 1E,F,H,L).

In an alternate counterstaining method, we detected myocardium with a *cardiac myosin light chain 2* (*cmlc2*) riboprobe (Yelon et al., 1999). In these embryos, we performed whole-mount in situ hybridization before detecting fluorescein. We used a standard protocol (Yelon et al., 1999), except for the incorporation of 175 μg/ml 5-Bromo-6-Chloro-3-Indolyl Phosphate (‘magenta-phos’; Sigma B-5667) as the substrate for the alkaline phosphatase reaction, generating a pink precipitate (Fig. 1G,I-K; Fig. 5L,M; Fig. 6E,F).

Scoring labeled cells

In each 44 hpf embryo, we assessed contributions of labeled cells to both the myocardium and endocardium of both cardiac chambers. We distinguished the atrium from the ventricle morphologically, relative to the constriction at the atrioventricular boundary. Morphological criteria also allowed us to distinguish myocardial cells, which are ovoid and tend to project circumferentially around the heart, from endocardial cells, which are more elongated and tend to project longitudinally. Additionally, we assessed colocalization of labeled cells with counterstained myocardium. To verify the accuracy of scoring myocardium and endocardium, we examined longitudinal sections through the heart in select embryos (e.g. Fig. 1F,H). Before cutting 5 μm sections, we dehydrated embryos through an ethanol series, cleared them in xylenes, and embedded them in paraffin.

When possible, we assessed contributions to non-cardiac lineages, based on morphology and location of labeled cells (Fig. 4A,C,E,G).

However, we were not able to score all lineages thoroughly: both pigmentation and MF20 staining in the somites obscured visualization of labeled cells, especially in the gut tube.

Whole-mount in situ hybridization and photography

Whole-mount in situ hybridization was performed as described previously (Yelon et al., 1999). We used antisense *cmlc2* (*Not*I, T7), *vmhc* (*Not*I, T7) and *amhc* (*Bgl*II, T7) probes (Yelon et al., 1999; Berdougo et al., 2003). We examined embryos with Zeiss M2Bio and Axioplan microscopes and photographed them with a Zeiss Axiocam digital camera. Images were processed with Zeiss AxioVision 3.0.6 and Adobe Photoshop 7.0 software.

Immunofluorescence

Whole-mount immunofluorescence was performed as described previously (Yelon et al., 1999). MF20 (Bader et al., 1982) and S46 (generous gift from F. Stockdale) monoclonal antibodies were detected with goat anti-mouse IgG2b-TRITC and goat anti-mouse IgG1-FITC secondary antibodies (Southern Biotechnology Associates), respectively.

RNA injection

We synthesized capped *lefty1* mRNA (Thisse and Thisse, 1999) using the SP6 mMessage mMachine system (Ambion) and injected embryos with both 1 pg mRNA and caged fluorescein at the one- to two-cell stage.

Results

Constructing a fate map of cardiac chamber progenitors at 40% epiboly

We investigated the locations of cardiac chamber progenitors in the zebrafish blastula at the 40% epiboly stage, just prior to the initiation of gastrulation. Previous studies at this stage have mapped the general location of cardiac progenitors, without analysis of chamber identity; in particular, Warga and Nüsslein-Volhard (Warga and Nüsslein-Volhard, 1999) have established that cardiac progenitors reside in the first four tiers of blastomeres (Fig. 1A, white arrows) adjacent to the embryonic margin (Fig. 1A, red arrowheads), in lateral regions 60-150° from the dorsal midline, on both the left and right sides of the embryo. Building on this foundation, we created a high-resolution map of the organization and density of chamber progenitors within these broadly defined lateral marginal zones.

A detailed description of our fate mapping strategy is provided in the Materials and methods. In brief, using laser-mediated activation of caged fluorescein, we labeled two or three neighboring blastomeres in each of 184 wild-type embryos. For each embryo, we recorded the latitude (Fig. 1A-C) and longitude (Fig. 1D) of the labeled cells. At 44 hours

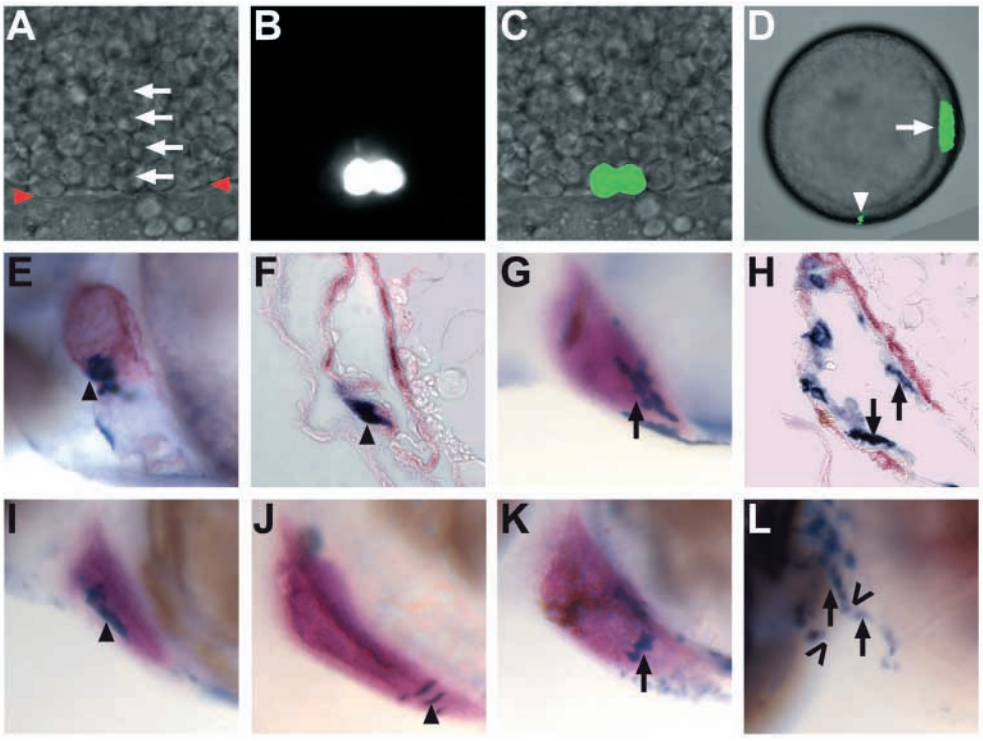

Fig. 1. Labeling chamber progenitors by activating caged fluorescein. (A) Lateral view of zebrafish blastula at 40% epiboly, animal pole to the top, dorsal to the right. Red arrowheads indicate the embryonic margin, where the blastoderm meets the yolk. Nuclei of the yolk syncytial layer are visible below the margin. White arrows demarcate blastomere tiers 1, 2, 3 and 4, counting up from the margin. (B) In this example, caged fluorescein is activated in 2 neighboring blastomeres. (C) Overlay of DIC image and fluorescent image, pseudocolored in green, demonstrates that the labeled blastomeres are in tier 1. (D) Animal view, dorsal towards the right. After incubation at 20°C for 1 hour, the longitudinal position of labeled cells (arrowhead) is recorded as an angular measurement around the circumference of the embryo, with the center of *Tg(gsc:gfp)* expression (arrow) defined as 0°. In this embryo, the labeled cells occupy positions 90-95° from dorsal. (E-L) Assessment of cardiac contributions at 44 hpf. Lateral views of the heart, anterior towards the left. Labeled myocardial (E,F,I,J) and endocardial (G,H,K,L) progeny are marked with a blue precipitate, and myocardium is counterstained with a pink precipitate (see Materials and methods). Identities of labeled cells are determined by morphology and location, either in whole mount (E,G,I-L) or in longitudinal sections (F,H). We show a series of typical results. (E) After labeling three blastomeres in tier 1, 105-115° from dorsal, we found six labeled cells in the ventricular myocardium (arrowhead). (F) Sectioning confirms the myocardial identity of the labeled cells in E (arrowhead). (G) After labeling two blastomeres in tier 4, 125-130°, we found multiple labeled cells in the atrial endocardium (arrow). (H) After labeling two blastomeres in tier 2, 88-93°, we found multiple clusters of labeled cells in the atrial endocardium, shown via sectioning (arrows). (I) After labeling 2 blastomeres in tier 1, 87-93°, we found six myocardial cells arranged along the long axis of the ventricle (arrowhead). (J) After labeling two blastomeres in tier 2, 122-128°, we found five myocardial cells arranged along the long axis of the atrium (arrowhead). (K) After labeling two blastomeres in tier 1, 110-118°, we found labeled cells in the ventricular endocardium (arrow). (L) After labeling two blastomeres in tier 2, 92-98°, we found a chain of endocardial cells extending from the atrium to the ventricle (arrows). Open arrowheads indicate the plane of the atrioventricular boundary.

post fertilization (hpf), we assessed the contribution of labeled cells to the myocardium and endocardium of the ventricle and atrium (Fig. 1E-L). Thus, by correlating cardiac contributions with initial positions of labeled blastomeres, we generated a fate map of chamber progenitors at 40% epiboly (Tables 1, 2; Figs 2, 3).

Spatial organization of ventricular and atrial myocardial progenitors

Consistent with previous studies (Warga and Nüsslein-Volhard, 1999), our fate map indicates that myocardial progenitors are located within the first four tiers of blastomeres, 60-140° from the dorsal midline, on both sides of the embryo (Table 1, Fig. 2B). (For convenience, we refer to these lateral marginal zones of the embryo as LMZs.) In each embryo containing labeled myocardium, labeled cells are either in the ventricle or the atrium; no embryos contain labeled myocardial cells in both chambers (Table 1, Fig. 2B). Typically, labeled myocardial cells are clustered within three cell diameters of each other (21/25 embryos with three to seven labeled myocardial cells; Fig. 1E,F,I,J). In many of these cases (13/21 embryos; Fig. 1I,J), groups of labeled cells are oriented along the long axis of the chamber. Even so, no groups of labeled cells span the atrioventricular boundary (Table 1, Fig. 2B). The failure to label both ventricular and atrial myocardium in a single embryo is consistent with prior work demonstrating early separation of ventricular and atrial lineages (Stainier et al., 1993).

The resolution of our fate map reveals a previously unrecognized spatial organization of ventricular and atrial myocardial progenitors. Ventricular progenitors tend to be found closer to the margin than do atrial progenitors (Table 1, Fig. 2B). Specifically, we find ventricular progenitors primarily in tiers 1 (11/48 experiments in tier 1) and 2 (7/57 experiments), rarely in tier 3 (1/53 experiments), and never in tier 4 (0/26 experiments). By contrast, atrial progenitors never originate in tier 1 (0/48 experiments) but are found in tiers 2 (4/57 experiments), 3 (4/53 experiments) and 4 (3/26 experiments). Furthermore, within tiers 2 and 3, ventricular progenitors tend to be located closer to the dorsal midline than are atrial progenitors: ventricular progenitors are found 60-

Table 1. Myocardial chamber progenitors

Tier	Angle	Side	Number of blastomeres labeled	Chamber	Number of progeny labeled
1	62-68	R	2	Ventricle	3
1	66-74	L	2	Ventricle	3
1	80-90	R	3	Ventricle+	3
1	82-86	R	2	Ventricle	4
1	85-95	L	3	Ventricle	10
1	85-105	R	5	Ventricle	6
1	87-93	L	2	Ventricle	6
1	87-95	R	2	Ventricle	3
1	100-110	R	3	Ventricle	2
1	105-115	L	3	Ventricle	6
1	105-120	L	5	Ventricle	5
1	105-125	L	5	Ventricle	4
1	110-116	L	2	Ventricle	2
1	118-127	L	2	Ventricle	4
1	125-145	L	5	Ventricle	2
2	62-68	L	2	Ventricle	2
2	75-80	R	2	Ventricle	5
2	86-93	R	2	Ventricle	4
2	92-97	L	2	Ventricle	6
2	97-103	L	2	Ventricle	5
2	106-112	L	2	Ventricle	5
2	112-120	L	2	Ventricle	6
3	89-95	R	2	Ventricle	4
2	92-98	L	2	Atrium+	6
2	94-106	L	2	Atrium	2
2	122-128	R	2	Atrium	5
2	128-135	L	2	Atrium	5
3	100-110	R	3	Atrium	3
3	105-110	L	3	Atrium	3
3	121-125	L	2	Atrium	6
3	130-140	R	3	Atrium	3
4	105-110	L	2	Atrium	3
4	105-110	L	2	Atrium	4
4	105-110	R	2	Atrium	5

Summary of experiments yielding myocardial progeny. Each row describes an individual embryo, indicating the latitude (tier), longitude (angle), number of blastomeres labeled, chamber contribution and number of labeled myocardial progeny. For blastomeres on the left (L) side of the embryo, longitude describes angular distance from dorsal in a clockwise direction. For blastomeres on the right (R) side of the embryo, longitude describes angular distance from dorsal in a counterclockwise direction. The two embryos with contribution to both myocardium and endocardium are labeled with '+'.

Table 2. Endocardial chamber progenitors

Tier	Angle	Side	Number of blastomeres labeled	Chamber
1	60-100	R	5	Ventricle
1	86-93	R	3	Ventricle
1	100-110	L	3	Ventricle
1	110-118	R	2	Ventricle
2	55-62	R	2	Ventricle
2	63-68	L	2	Ventricle
2	69-76	R	2	Ventricle
2	78-82	L	2	Ventricle
2	88-93	R	2	Ventricle
2	89-95	L	2	Ventricle
2	126-128	L	2	Ventricle
3	84-92	L	2	Ventricle
4	85-90	L	2	Ventricle
1	117-122	R	2	Atrium
1	134-140	R	2	Atrium
2	92-98	L	2	Atrium+
2	120-125	R	2	Atrium
3	85-95	L	3	Atrium
4	55-60	L	2	Atrium
4	125-130	R	2	Atrium
4	125-130	L	2	Atrium
1	80-86	L	2	Ventricle/atrium
1	80-90	R	3	Ventricle/atrium+
2	74-79	R	2	Ventricle/atrium
2	86-92	R	2	Ventricle/atrium
2	92-98	L	2	Ventricle/atrium
2	97-103	R	2	Ventricle/atrium
2	110-115	R	2	Ventricle/atrium
2	112-117	R	2	Ventricle/atrium
2	119-125	L	2	Ventricle/atrium
2	125-131	R	2	Ventricle/atrium
2	132-139	R	2	Ventricle/atrium
3	72-78	L	2	Ventricle/atrium
3	99-106	R	2	Ventricle/atrium
3	104-110	R	2	Ventricle/atrium
3	100-110	R	3	Ventricle/atrium
4	105-110	L	2	Ventricle/atrium
4	115-120	R	2	Ventricle/atrium

Summary of experiments yielding endocardial progeny. Each row describes an individual embryo, as described for Table 1. The two embryos with contribution to both myocardium and endocardium are labeled with a plus (+).

125° from dorsal, and atrial progenitors are found 90-140° from dorsal (Fig. 2B).

In addition to establishing the spatial relationships of ventricular and atrial progenitors, our data provide an estimate of the density of myocardial progenitors in the blastula. Labeling 2 neighboring blastomeres within the LMZs produces myocardial progeny in ~20% (23/115) of experiments, suggesting a relatively sparse distribution of individual myocardial progenitors (Fig. 2B). In these experiments, the number of labeled myocardial cells ranges from two to six, with an average of 4.3 labeled myocardial cells per embryo (Table 1), suggesting that an average myocardial progenitor produces four myocardial progeny by 44 hpf. In this regard, it is interesting to note that experiments labeling three blastomeres and experiments labeling five blastomeres also yield an average of 4.3 labeled myocardial cells, just as in experiments labeling 2 blastomeres (Table 1). The consistency of the average myocardial output, regardless of the initial number of labeled blastomeres, lends further support to the notion that individual myocardial progenitors are spread at a low density, rather than tightly clustered, within the LMZs.

Intermingling of ventricular and atrial endocardial progenitors

As in previous work (Warga and Nüsslein-Volhard, 1999), we find endocardial progenitors in the same LMZs as myocardial progenitors (Table 2, Fig. 3). However, in contrast to myocardial progenitors, ventricular and atrial endocardial progenitors are found throughout the LMZs without apparent organization. Both ventricular and atrial endocardial progenitors are found in all four tiers and over the entire 60-140° range (Table 2, Fig. 3). Furthermore, and also in contrast to our data for myocardial progenitors, in many (17/37) experiments, labeled endocardial cells are found in both cardiac chambers (Table 2, Fig. 3). In most (34/37) experiments, labeled endocardial cells are grouped together within the heart tube (Fig. 1G,K,L). Embryos with labeled cells in both ventricular and atrial endocardium are especially interesting: in most (14/17) of these cases, a chain of labeled endocardial cells extends across the atrioventricular boundary (Fig. 1L).

As with myocardial progenitors, our data indicate the frequency of labeling endocardial progenitors at 40% epiboly. When labeling two neighboring blastomeres in the LMZs, ~28% (32/115) of embryos contain labeled endocardial cells (Fig. 3). Owing to the difficulty of discerning endocardial cell boundaries, especially in contiguous chains of cells, it is challenging to determine the number of labeled endocardial cells reliably; in scoreable cases, the number of labeled endocardial cells per embryo ranged from two to 20.

Multiple lineages arise from the lateral marginal zone

Supporting and extending previous fate maps, our data indicate that cardiac chamber progenitors are intermingled with progenitors of other lineages in the LMZs (Kimmel et al., 1990; Warga and Nüsslein-Volhard, 1999). These other lineages include endoderm, endothelium, pectoral fin mesenchyme, blood, head muscle and pharyngeal tissue (Fig. 4) (Warga and Nüsslein-Volhard, 1999). Although our protocol is not optimal for analysis of all organs (see Materials and methods), we were often able to score contribution of labeled cells to head vessels, circulating blood, pharyngeal pouches

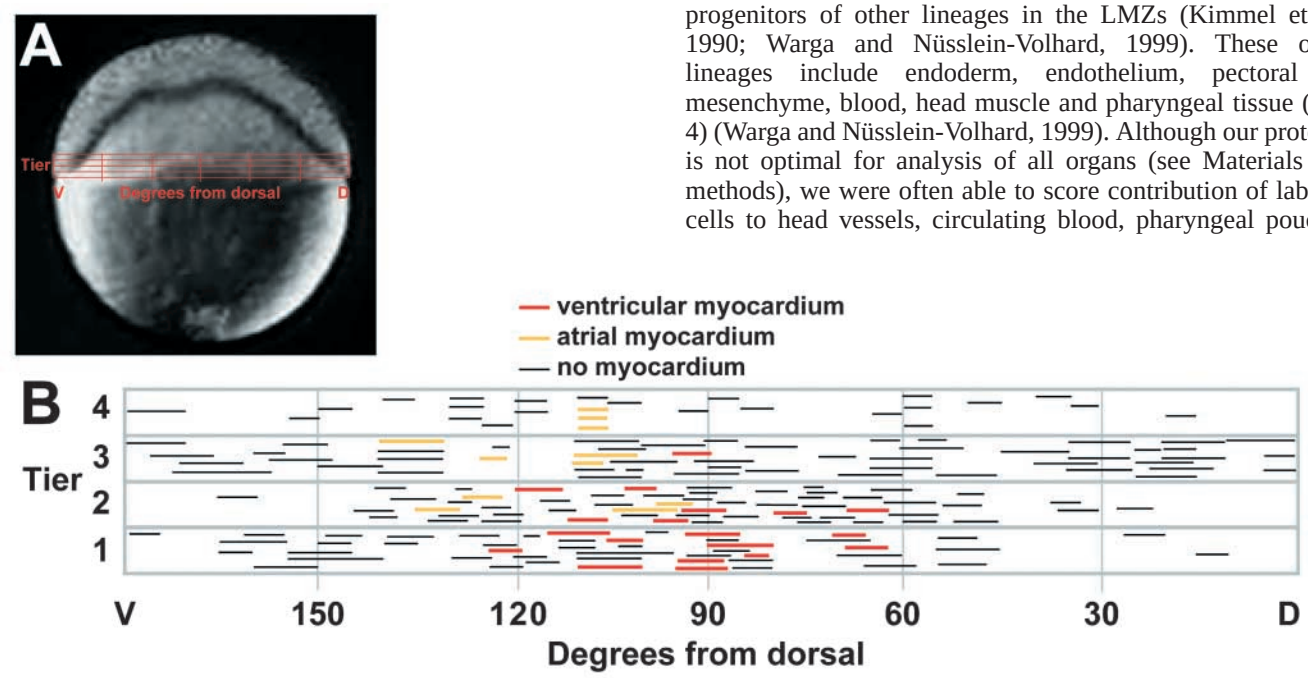

Fig. 2. Ventricular and atrial myocardial progenitors are spatially organized at 40% epiboly. (A) The coordinates of our fate map projected onto a lateral view at 40% epiboly; background image adapted, with permission, from Karlstrom and Kane (Karlstrom and Kane, 1996). Latitude, on the vertical axis, is expressed in tiers, or cell diameters, from the margin. Longitude, on the horizontal axis, is expressed in degrees around the circumference of the embryo, with the center of *Tg(gsc:gfp)* expression defined as 0°. (B) Fate map of myocardial chamber progenitors. Each horizontal bar represents an individual experimental embryo. The position of a bar on the map corresponds with the location of labeled blastomeres. Bar color indicates myocardial contribution of labeled cells: red, contribution to ventricular myocardium; yellow, contribution to atrial myocardium; black, no myocardial progeny. All data from Table 1, except for experiments labeling five blastomeres, are included. As progenitor distribution, chamber contribution and density appear equivalent on both the left and right sides of the embryo (Table 1), the data are summarized together in the fate map. Compiling all data, ventricular myocardial progenitors are found 60-125° from dorsal in tiers 1, 2 and 3. By contrast, atrial myocardial progenitors are found 90-140° from dorsal in tiers 2, 3 and 4.

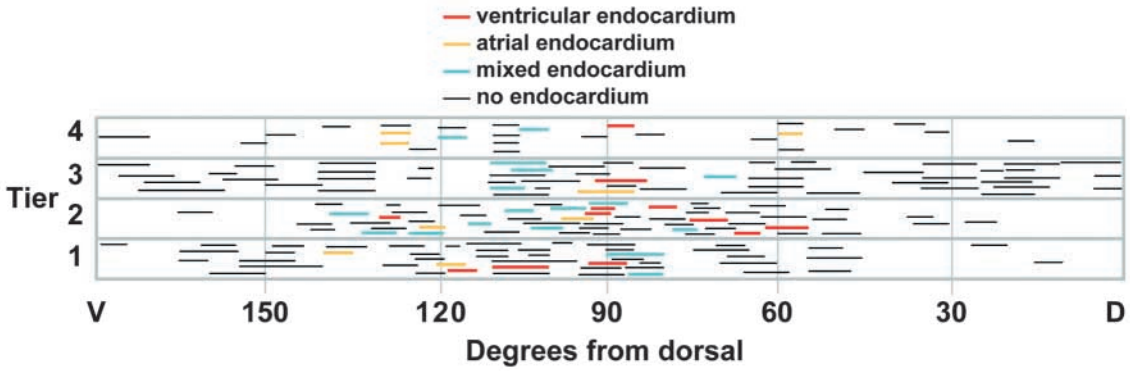

Fig. 3. Ventricular and atrial endocardial progenitors are intermingled at 40% epiboly. The fate map of endocardial chamber progenitors is depicted as described for the myocardial fate map (Fig. 2B). In this map, bar colors correspond to the endocardial contribution of labeled cells: red, contribution to ventricular endocardium; yellow, contribution to atrial endocardium; cyan, contribution to both ventricular and atrial endocardium; black, no endocardial progeny. All data from Table 2, except for the experiment labeling five blastomeres, are included. Endocardial progenitors are found 55-140° from dorsal in all four tiers.

and pectoral fin mesenchyme (Fig. 4). We find progenitors of head vessels, pharyngeal pouches and fin mesenchyme in locations compatible with and in addition to those noted in other studies (Fig. 4B,E,H) (Warga and Nüsslein-Volhard, 1999). We also find a previously unreported population of blood progenitors in tiers 1 and 2, 45-100° from dorsal (Fig. 4D). Some blastomeres in this area give rise to circulating cells in cephalic regions; based on their location and morphology, these progeny are probably myeloid cells, most likely macrophages known to reside in a region of LPM anterior to the myocardial precursors (Herbomel et al., 1999; Herbomel et al., 2001; Lieschke et al., 2002).

Location prior to gastrulation correlates with location in lateral plate mesoderm

Despite the intermingling of multiple mesendodermal lineages in the LMZs, our fate map suggests that ventricular and atrial myocardial progenitors might remain relatively organized during and following gastrulation. To explore this model, we examined whether blastomeres from distinct regions of the LMZs migrate to particular regions of the LPM. Specifically, we compared the destinations of LMZ blastomeres from a dorsal portion of tier 1 with those from a ventral region of tier 3 (Fig. 5A-H). At the end of gastrulation (tailbud stage, 10 hpf), we found that blastomeres from 60-100° of tier 1 contribute to

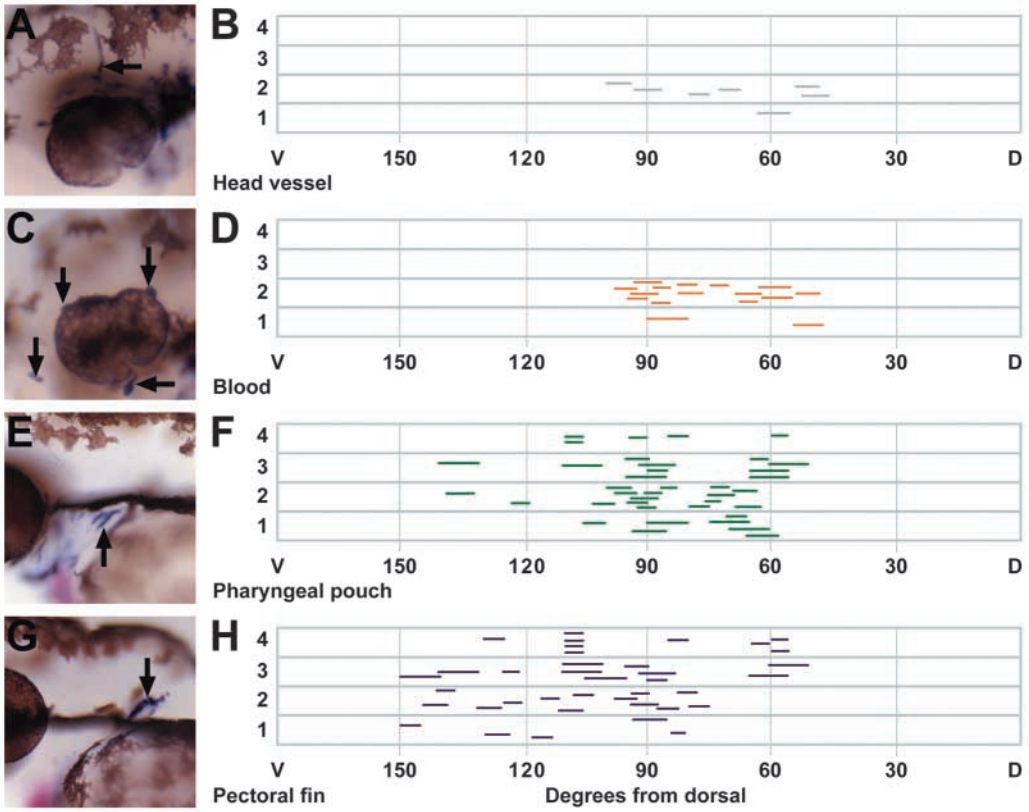

Fig. 4. Multiple lineages arise from the lateral marginal zone. Although we did not score non-cardiac lineages thoroughly, we noted the origins of some frequently detected cell types. (A,C,E,G) Lateral views at 44 hpf, anterior towards the left, showing examples of labeled cells (arrows). (B,D,F,H) Fate maps indicating experiments in which labeled blastomeres gave rise to head vessels, circulating blood cells in cranial locations, pharyngeal pouches or pectoral fin mesenchyme. Progenitors for head endothelium (A,B) and presumed myeloid cells (C,D) are found 45-100° from dorsal in tiers 1 and 2. Progenitors for pharyngeal pouches (E,F) and pectoral fin mesenchyme (G,H) are found 50-150° from dorsal in tiers 1-4.

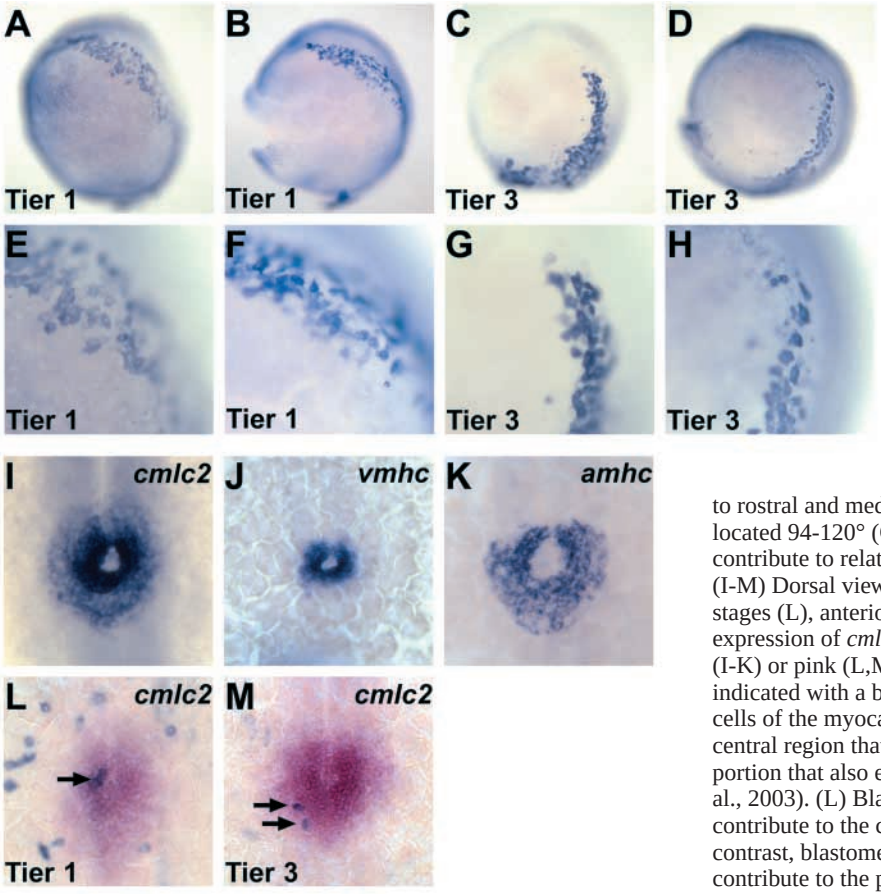

Fig. 5. Progenitor location prior to gastrulation correlates with location of progeny in LPM. (A-D) Lateral views at tailbud stage, rostral towards the top. Blue precipitate indicates locations of cells derived from labeled blastomeres. (E-H) Higher magnification views of embryos shown in (A-D). Blastomeres located 62-86° (A,E) or 67-95° (B,F) from dorsal in tier 1 contribute to rostral and medial regions of the LPM. By contrast, blastomeres located 94-120° (C,G) or 120-144° (D,H) from dorsal in tier 3 contribute to relatively caudal and lateral regions of the LPM. (I-M) Dorsal views of embryos at 22 somites (I-K,M) and 20 somites stages (L), anterior towards the top. In situ hybridization indicates expression of *cmlc2* (I,L,M), *vmhc* (J),and *amhc* (K) with a blue (I-K) or pink (L,M) precipitate. Progeny of labeled blastomeres are indicated with a blue precipitate (L,M). *cmlc2* is expressed in all cells of the myocardial cone (I), with more robust expression in the central region that also expresses *vmhc* (J) than in the peripheral portion that also expresses *amhc* (K) (Yelon et al., 1999; Berdougo et al., 2003). (L) Blastomeres located 101-107° from dorsal in tier 1 contribute to the central region of the myocardial cone. (M) By contrast, blastomeres located 110-116° from dorsal in tier 3 contribute to the peripheral region of the myocardial cone.

a rostral and medial portion of the LPM (*n*=4; Fig. 5A,B,E,F). By contrast, blastomeres from 100-140° of tier 3 contribute to a relatively caudal and lateral portion of the LPM (*n*=5; Fig. 5C,D,G,H).

Extending this analysis further, we assessed positions of labeled cells as the heart tube begins to form (20-22 somites, 19-20 hpf). At this stage, the LPM has migrated towards the embryonic midline, allowing bilateral populations of myocardial cells to meet and form a shallow cone (Yelon et al., 1999). Expression patterns of chamber-specific genes suggest that the central region of the cone, expressing *ventricular myosin heavy chain* (*vmhc*), will form the ventricle; and that the peripheral portion of the cone, expressing *atrial myosin heavy chain* (*amhc*), will form the atrium (Fig. 5I-K) (Berdougo et al., 2003; Yelon et al., 1999). Correspondingly, myocardial progenitors from tier 1 contribute to the central portion of the cone (*n*=5; Fig. 5L). Furthermore, myocardial progenitors from a ventral portion of tier 3 contribute to the peripheral portion of the cone (*n*=2; Fig. 5M).

Together, these results demonstrate that ventricular and atrial myocardial progenitors retain their relative organization from blastula stages through heart tube formation. In the blastula, ventricular and atrial progenitors occupy different regions of the LMZs, with ventricular progenitors located more marginally and dorsally than are atrial progenitors (Fig. 2B). As gastrulation proceeds, blastomeres from different regions of the LMZs form different regions of the LPM, with presumed ventricular progenitors located more rostrally and medially than presumed atrial progenitors (Fig. 5A-H). Finally, relative orientation within the LPM remains consistent as heart tube assembly proceeds, with medial cells contributing to the future ventricle and lateral cells contributing to the future atrium (Fig. 5I-M).

Nodal signaling promotes ventricular specification

Our fate map demonstrates that myocardial progenitors are spatially organized prior to gastrulation; however, it does not indicate when chamber fates are specified. Nevertheless, the relative positions of ventricular and atrial progenitors suggest that differential reception of secreted signals could influence chamber fate. For example, ventricular progenitors would have preferential exposure to signals that are found at the margin or in a vegetal-animal gradient. In the zebrafish blastula, Cyclops and Squint, members of the Nodal family of TGFβ-related ligands, are generated in marginal blastomeres and the yolk syncytial layer (Erter et al., 1998; Feldman et al., 1998; Rebagliati et al., 1998a; Rebagliati et al., 1998b; Sampath et al., 1998). Furthermore, zebrafish Nodal signals have been shown to influence cell fate relative to distance from the margin, particularly in the dorsal mesoderm (Chen and Schier, 2001; Dougan et al., 2003; Gritsman et al., 2000). Therefore, we hypothesized that Nodal signaling could regulate chamber fate specification.

Prior studies have established that complete inhibition of Nodal signaling in the zebrafish embryo blocks specification of all mesendodermal lineages at the blastula margin, resulting

in the elimination of cardiac mesoderm (Carmany-Rampey and Schier, 2001; Chen and Schier, 2001; Feldman et al., 1998; Gritsman et al., 1999; Thisse and Thisse, 1999). Partial reduction of Nodal signaling, as in zebrafish mutants lacking zygotic supplies of the EGF-CFC co-receptor One-eyed pinhead (Oep), causes a variable loss of myocardium, with the ventricle tending to be more significantly affected than the atrium (Reiter et al., 2001). Nodal signaling can also be inhibited by the extracellular antagonist Lefty1 (Chen and Schier, 2002; Cheng et al., 2004; Thisse and Thisse, 1999). Fittingly, we find that embryos ectopically expressing low levels of *lefty1* exhibit variable reductions of myocardium, with preferential loss of ventricular myocardium (Fig. 6A-D); the range of cardiac phenotypes observed mimics that found in zygotic *oep* mutants (Reiter et al., 2001). These phenotypes implicate Nodal signaling in ventricular development, but they fail to establish its precise role. Nodal signaling may promote ventricular fate specification; alternatively, Nodal signaling could play a later role in promoting ventricular differentiation, growth, or survival.

To clarify the role of Nodal signaling in ventricle formation, we examined alterations to the myocardial fate map in embryos injected with *lefty1* mRNA. To detect a shift in the vegetal-animal distribution of fates, we focused our analysis on tier 1, where wild-type myocardial progenitors are exclusively ventricular (Fig. 2B). In these experiments, we typically labeled multiple adjacent blastomeres, in order to facilitate a rapid survey of resident progenitors. We detected myocardial progeny in 24% (7/29) of the *lefty1*-injected embryos in which we labeled tier 1 LMZ blastomeres (Fig. 6G). In a striking contrast to our wild-type fate map, we find both atrial and ventricular progenitors in tier 1 of *lefty1*-injected embryos (Fig. 6E-G), indicating a fate transformation of tier 1 blastomeres when Nodal signaling is antagonized. Therefore, Nodal signaling contributes to the vegetal-animal patterning of myocardial progenitors, promoting the assignment of ventricular fate in blastomeres near the embryonic margin.

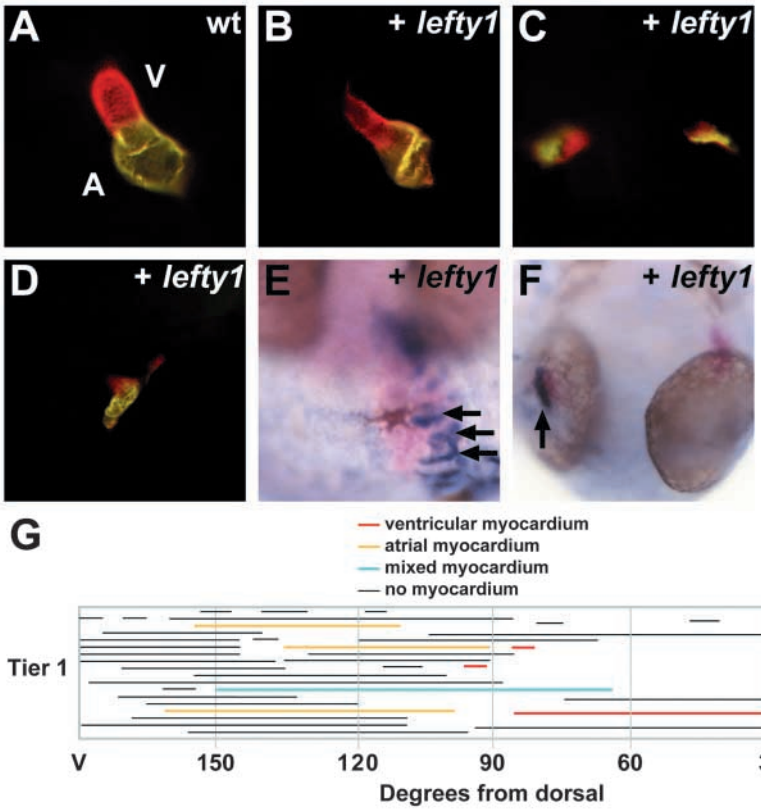

Fig. 6. Antagonism of Nodal signaling alters myocardial fate assignment in tier 1 blastomeres. (A-D) Whole-mount immunofluorescence with the anti-myosin heavy chain monoclonal antibodies MF20 (TRITC) and S46 (FITC) at 36 hpf. (A,B,D) Lateral views, anterior towards the left. (C) Dorsal view, anterior towards the top. (A) In wild-type (wt) embryos, double exposure indicates MF20 staining in the ventricle (red, V), and overlap of MF20 and S46 staining in the atrium (yellow, A). In embryos injected with small amounts of *lefty1* mRNA (B-D), we observe variable reduction of myocardium, ranging from a moderately reduced ventricle and a subtly affected atrium (B) to severe reductions of ventricular tissue together with significant reductions of atrial tissue (C,D). In addition, ectopic expression of *lefty1* can disrupt endoderm formation, causing cardia bifida as shown in C (Yelon, 2001). (E,F) Examples of myocardial contributions by tier 1 blastomeres in embryos injected with *lefty1*. Labeled myocardial cells (blue precipitate) are examined with reference to an atrium-specific marker, *amhc* (pink precipitate) (Berdougo et al., 2003). (E) Frontal view at 36 hpf, dorsal towards the top. The amount of myocardium present resembles that in the embryo depicted in B. In this embryo, blastomeres located 65-150° from dorsal in tier 1 contributed to both atrial myocardium (arrows) and ventricular myocardium (below eyes and out of focal plane). (F) Dorsal view at 36 hpf, anterior towards the top. The amount of myocardium present resembles that in the embryo depicted in C. In this embryo, blastomeres located 90-135° from dorsal in tier 1 contributed to atrial myocardium (arrow). (G) Fate map of myocardial chamber progenitors in embryos injected with *lefty1*. Data are depicted as described for the myocardial fate map (Fig. 2B), except that experiments were performed only in tier 1. In this map, bar colors correspond to the myocardial contribution of labeled cells: red, contribution to ventricular myocardium; yellow, contribution to atrial myocardium; cyan, contribution to both ventricular and atrial myocardium; black, no myocardial progeny. When Nodal signaling is antagonized, both ventricular and atrial myocardial progenitors reside in tier 1. The dorsoventral organization of these progenitors roughly resembles that observed in tiers 2 and 3 of the wild-type fate map (Fig. 2), in that blastomeres located more dorsally than 125° give rise to ventricular myocardium and blastomeres located more ventrally than 90° give rise to atrial myocardium.

Discussion

Organization of cardiac chamber progenitors

Our fate map reveals the density and organization of myocardial and endocardial chamber progenitors within the zebrafish blastula at 40% epiboly. Both myocardial and endocardial progenitors reside within the LMZs, together with the progenitors of other mesendodermal lineages. The frequencies of detecting myocardial and endocardial progeny in our experiments indicate that at least 10% of LMZ blastomeres contribute to the myocardium and at least 14% of LMZ blastomeres contribute to the

endocardium. These figures, which are based on the assumption that we have labeled only one cardiac progenitor per experiment, are likely to be underestimates. Additional cardiac progenitors could reside in areas outside of the scope of our fate map, such as deeper layers of the DEL, or regions outside the LMZs, such as cardiac neural crest (Li et al., 2003; Sato and Yost, 2003).

Strikingly, our data show that myocardial and endocardial progenitor populations are organized considerably differently. Myocardial chamber progenitors are spatially organized at 40% epiboly; by contrast, endocardial chamber progenitors are distributed without apparent organization. In general, ventricular myocardial progenitors are located more marginally and dorsally than are atrial myocardial progenitors, although there is a zone of overlap in which both ventricular and atrial myocardial progenitors can be found (Fig. 7A). Nevertheless, none of our experiments in wild-type embryos yielded myocardial progeny in both the ventricle and atrium. Thus, ventricular and atrial myocardial lineages are clearly separated by 40% epiboly. This lineage separation could be the consequence of early patterning events that initiate chamber specification. Alternatively, lineage separation could be facilitated by orderly migration of LMZ blastomeres, preserving the relative orientation of ventricular and atrial progenitors until chamber specification occurs. Our data suggest that both scenarios – orderly migration and early patterning – apply to the myocardial progenitors.

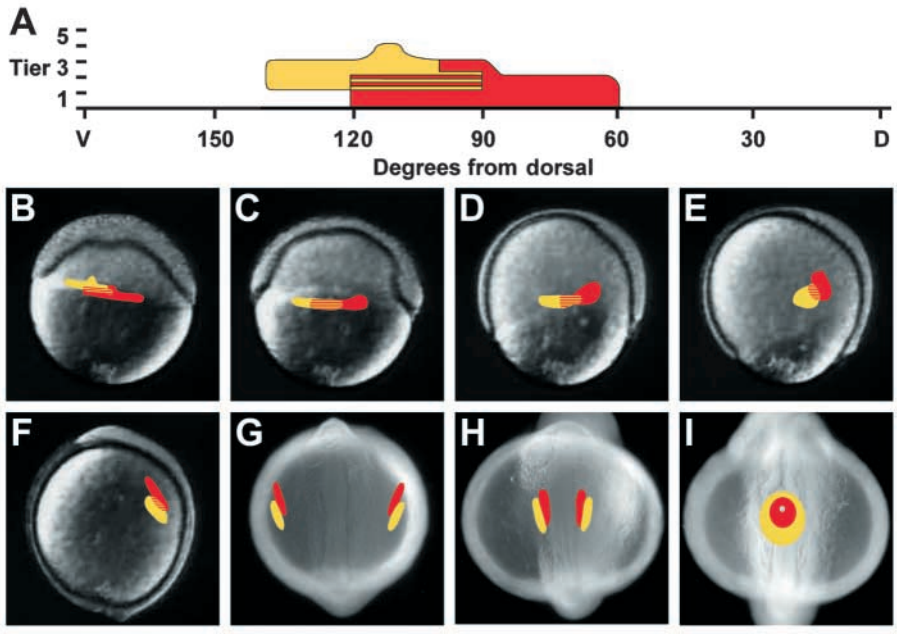

Fig. 7. Model of myocardial morphogenesis. The spatial organization of myocardial chamber progenitors at 40% epiboly and the locations of their progeny at tailbud and mid-somitogenesis stages suggest orderly migration of these populations. (A-I) Schematic representations of zones containing ventricular myocardial progenitors (red) or atrial myocardial progenitors (yellow). Zones containing both ventricular and atrial progenitors are depicted in red and yellow stripes. (A) Representation of myocardial fate map at 40% epiboly; primary data shown in Fig. 2B. (B-F) Frames from an animated model of myocardial morphogenesis (see Movie 1 at http://dev.biologists.org/supplemental); lateral views, dorsal towards the right, at (B) 40% epiboly, (C) shield, (D) 70% epiboly, (E) 85% epiboly and (F) tailbud stages. Background images adapted, with permission, from Karlstrom and Kane (Karlstrom and Kane, 1996). (G-I) Dorsal views, anterior towards the top, depicting myocardial progenitor zones within the LPM at (G) 5 somites, (H) 15 somites and (I) 22 somites.

Myocardial morphogenesis proceeds in an orderly fashion

Our finding that ventricular and atrial myocardial progenitors retain their relative orientation after gastrulation suggests that, although myocardial progenitors migrate substantially, there is little mixing between ventricular and atrial populations. Combining our observations with previous studies of LMZ blastomere movements (Myers et al., 2002; Sepich et al., 2000; Warga and Kimmel, 1990), we can predict the general locations of myocardial chamber progenitors during cardiac morphogenesis (Fig. 7B-I; see Movie 1 at http://dev.biologists.org/supplemental).

When gastrulation begins, the blastomeres closest to the margin involute first, followed by the higher tiers (Fig. 7B,C) (Warga and Kimmel, 1990). Thus, in the hypoblast, ventricular progenitors would tend to be slightly more rostral than are atrial progenitors. Additionally, by virtue of their initial dorsal positions, ventricular progenitors would be closer to the embryonic midline than are atrial progenitors. Subsequently, through convergence and extension, the wide zones containing myocardial progenitors become more narrow and extend rostrally (Fig. 7D-F) (Myers et al., 2002; Sepich et al., 2000). After gastrulation, myocardial chamber progenitors occupy discrete regions of the LPM (Fig. 7F,G). During somitogenesis stages, these bilateral populations migrate medially and eventually fuse to form the ventricular and atrial regions of the heart tube (Fig. 7G-I) (Yelon et al., 1999). Thus, our data are consistent with a generally orderly process of myocardial morphogenesis. In this regard, our findings are comparable to fate maps of other zebrafish germ layers: in particular, zebrafish neural and endodermal fate maps suggest early organization and orderly migration of tissue progenitors during gastrulation (Kozlowski et al., 1997; Warga and Nüsslein-Volhard, 1999; Woo et al., 1995).

It is interesting to compare the organization and morphogenesis of myocardial progenitors in zebrafish and chick. The initial organization of zebrafish myocardial progenitors places the ventricular progenitors closer to both the margin and the dorsal organizer; similarly, avian fate maps indicate a tendency of ventricular progenitors to involute earlier and closer to the node than atrial progenitors (Garcia-Martinez and Schoenwolf, 1993; Rosenquist, 1970). However, although their initial organization seems comparable, the orderly movements of zebrafish myocardial progenitors may not resemble the migration patterns of chamber progenitors in

chick. Although some early cell labeling studies in chick have suggested relatively coherent movements of groups of progenitors (Rosenquist, 1966; Stalsberg and DeHaan, 1969), other analyses suggest that chamber progenitors can move and intermix relatively freely until cardiac crescent formation is complete (DeHaan, 1963; Redkar et al., 2001).

In contrast to the orderly morphogenesis of myocardial progenitors, zebrafish endocardial progenitors are likely to intermix substantially during their migration into the heart tube. During somitogenesis stages, endocardial cells are thought to aggregate near the embryonic midline, at the future center of the myocardial cone (Stainier et al., 1993). Once the cone forms, the endocardial cells are then in position to generate the lining of the heart tube. This model, which is consistent with our data, suggests that endocardial chamber progenitors do not become spatially organized until they leave the midline to occupy a cardiac chamber; furthermore, it is possible that endocardial chamber lineages are not specified until chambers form. The high frequency of labeling both ventricular and atrial endocardial cells in our fate map suggests that these lineages are not separate at 40% epiboly (Fig. 3). Additionally, the observed chains of endocardial cells extending into both chambers (Fig. 1L) suggest clonal relationships of labeled cells in these experiments.

Nodal signaling patterns myocardial chamber progenitors

The vegetal-animal organization of myocardial chamber progenitors at 40% epiboly suggests that vegetal-animal signaling gradients could influence chamber specification. We demonstrate that ectopic expression of *lefty1* influences myocardial fate assignments in tier 1 blastomeres. Given that Lefty antagonizes the function of EGF-CFC-co-receptor-dependent TGFβ molecules (Chen and Schier, 2002; Cheng et al., 2004), it is likely that our data reflect endogenous roles of the Nodal ligands Squint and/or Cyclops in the zebrafish blastula (Erter et al., 1998; Feldman et al., 1998; Rebagliati et al., 1998a; Rebagliati et al., 1998b; Sampath et al., 1998). Previous studies have shown that elimination of Nodal signaling alters the fate map of the blastula margin, such that marginal fates, including myocardium, are completely absent; and ectodermal fates, which are normally found in higher tiers, are found in marginal locations (Carmany-Rampey and Schier, 2001; Dougan et al., 2003; Feldman et al., 2000). Our data indicate that reduction, rather than elimination, of Nodal signaling creates a finer vegetal-animal adjustment in fate assignments within the tiers of the LMZs, causing the distribution of ventricular and atrial myocardial progenitors in tier 1 to resemble the dorsoventral organization observed in tier 2 or 3 of the wild-type fate map. These data are reminiscent of the prior observation that reduced Nodal signaling causes fate transformations at the dorsal margin, such that notochord progenitors, normally located in tier 3 or higher, are found in tiers 1 and 2 (Gritsman et al., 2000). Although our results do not indicate how directly Nodal signaling influences myocardial patterning, our data are congruent with a general model in which reduction of Nodal signaling influences the entire blastula margin, shifting relatively animal fate assignments to more vegetal positions (Carmany-Rampey and Schier, 2001; Dougan et al., 2003).

Our data clearly demonstrate the impact of Nodal signaling on chamber specification; however, the Nodal pathway is unlikely to be the sole regulator of this process. In particular, our fate map suggests that chamber fate assignment could be accomplished through an intersection of vegetal-animal and dorsal-ventral patterning. In the zebrafish blastula, Bmp, Wnt and Fgf signals all regulate aspects of dorsal-ventral patterning (Schier, 2001). Future studies examining the influences of these signaling pathways on the myocardial fate map are therefore likely to provide additional insight regarding the integrated network of signals that pattern the myocardial progenitors.

We thank S. Zimmerman, T. Bruno and N. Dillon for excellent fish care; A. Schier, A. Joyner, C. Rushlow, M. Frasch, L. Solnica-Krezel, J. Feldman, and members of the Yelon and Schier laboratories for valuable discussions; A. Carmany-Rampey for help with fate mapping protocols; and B. Nowak for technical help with uncaging equipment. B.R.K. is supported by the MSTP of NYU School of Medicine and the NYU Graduate Training Program in Developmental Genetics (T32HD07520). This work is supported by the NIH (RO1 HL69594 to D.Y.).

References

Bader, D., Masaki, T. and Fischman, D. A. (1982). Immunochemical analysis of myosin heavy chain during avian myogenesis *in vivo* and *in vitro*. *J. Cell Biol.* **95**, 763-770.

Bao, Z. Z., Bruneau, B. G., Seidman, J. G., Seidman, C. E. and Cepko, C. L. (1999). Regulation of chamber-specific gene expression in the developing heart by Irx4. *Science* **283**, 1161-1164.

Berdougo, E., Coleman, H., Lee, D. H., Stainier, D. Y. and Yelon, D. (2003). Mutation of *weak atrium/atrial myosin heavy chain* disrupts atrial function and influences ventricular morphogenesis in zebrafish. *Development* **130**, 6121-6129.

Bisaha, J. G. and Bader, D. (1991). Identification and characterization of a ventricular-specific avian myosin heavy chain, VMHC1: expression in differentiating cardiac and skeletal muscle. *Dev. Biol.* **148**, 355-364.

Bruneau, B. G., Bao, Z.-Z., Tanaka, M., Schott, J.-J., Izumo, S., Cepko, C. L., Seidman, J. G. and Seidman, C. E. (2000). Cardiac expression of the ventricle-specific homeobox gene *Irx4* is modulated by Nkx2-5 and dHand. *Dev. Biol.* **217**, 266-277.

Carmany-Rampey, A. and Schier, A. F. (2001). Single-cell internalization during zebrafish gastrulation. *Curr. Biol.* **11**, 1261-1265.

Chen, Y. and Schier, A. F. (2001). The zebrafish Nodal signal Squint functions as a morphogen. *Nature* **411**, 607-610.

Chen, Y. and Schier, A. F. (2002). Lefty proteins are long-range inhibitors of Squint-mediated nodal signaling. *Curr. Biol.* **12**, 2124-2128.

Cheng, S. K., Olale, F., Brivanlou, A. H. and Schier, A. F. (2004). Lefty blocks a subset of TGF-β signals by antagonizing EGF-CFC coreceptors. *PLoS Biol.* **2**, 215-226.

DeHaan, R. L. (1963). Migration patterns of the precardiac mesoderm in the early chick embryo. *Exp. Cell. Res.* **29**, 544-560.

DeHaan, R. L. (1965). Morphogenesis of the vertebrate heart. In *Organogenesis* (ed. R. L. DeHaan and H. Ursprung), pp. 377-419. New York: Holt, Rinehart and Winston.

Doitsidou, M., Reichman-Fried, M., Stebler, J., Koprunner, M., Dorries, J., Meyer, D., Esguerra, C. V., Leung, T. and Raz, E. (2002). Guidance of primordial germ cell migration by the chemokine SDF-1. *Cell* **111**, 647-659.

Dougan, S. T., Warga, R. M., Kane, D. A., Schier, A. F. and Talbot, W. S. (2003). The role of the zebrafish nodal-related genes *squint* and *cyclops* in patterning of mesendoderm. *Development* **130**, 1837-1851.

Erter, C. E., Solnica-Krezel, L. and Wright, C. V. (1998). Zebrafish *nodal-related 2* encodes an early mesendodermal inducer signaling from the extraembryonic yolk syncytial layer. *Dev. Biol.* **204**, 361-372.

Feldman, B., Gates, M. A., Egan, E. S., Dougan, S. T., Rennebeck, G., Sirotkin, H. I., Schier, A. F. and Talbot, W. S. (1998). Zebrafish organizer development and germ-layer formation require nodal-related signals. *Nature* **395**, 181-185.

Feldman, B., Dougan, S. T., Schier, A. F. and Talbot, W. S. (2000). Nodal-

related signals establish mesendodermal fate and trunk neural identity in zebrafish. *Curr. Biol.* **10**, 531-534.
Garcia-Martinez, V. and Schoenwolf, G. C. (1993). Primitive-streak origin of the cardiovascular system in avian embryos. *Dev. Biol.* **159**, 706-719.
Gritsman, K., Zhang, J., Cheng, S., Heckscher, E., Talbot, W. S. and Schier, A. F. (1999). The EGF-CFC protein one-eyed pinhead is essential for nodal signaling. *Cell* **97**, 121-132.
Gritsman, K., Talbot, W. S. and Schier, A. F. (2000). Nodal signaling patterns the organizer. *Development* **127**, 921-932.
Herbomel, P., Thisse, B. and Thisse, C. (1999). Ontogeny and behaviour of early macrophages in the zebrafish embryo. *Development* **126**, 3735-3745.
Herbomel, P., Thisse, B. and Thisse, C. (2001). Zebrafish early macrophages colonize cephalic mesenchyme and developing brain, retina, and epidermis through a M-CSF receptor-dependent invasive process. *Dev. Biol.* **238**, 274-288.
Hochgreb, T., Linhares, V. L., Menezes, D. C., Sampaio, A. C., Yan, C. Y., Cardoso, W. V., Rosenthal, N. and Xavier-Neto, J. (2003). A caudorostral wave of RALDH2 conveys anteroposterior information to the cardiac field. *Development* **130**, 5363-5374.
Karlstrom, R. O. and Kane, D. A. (1996). A flipbook of zebrafish embryogenesis. *Development Suppl.*, 461.
Kimmel, C. B., Ballard, W. W., Kimmel, S. R., Ullmann, B. and Schilling, T. F. (1995). Stages of embryonic development of the zebrafish. *Dev. Dyn.* **203**, 253-310.
Kimmel, C. B., Warga, R. M. and Schilling, T. F. (1990). Origin and organization of the zebrafish fate map. *Development* **108**, 581-594.
Kozlowski, D. J., Murakami, T., Ho, R. K. and Weinberg, E. S. (1997). Regional cell movement and tissue patterning in the zebrafish embryo revealed by fate mapping with caged fluorescein. *Biochem. Cell Biol.* **75**, 551-562.
Li, Y. X., Zdanowicz, M., Young, L., Kumiski, D., Leatherbury, L. and Kirby, M. L. (2003). Cardiac neural crest in zebrafish embryos contributes to myocardial cell lineage and early heart function. *Dev. Dyn.* **226**, 540-550.
Lieschke, G. J., Oates, A. C., Paw, B. H., Thompson, M. A., Hall, N. E., Ward, A. C., Ho, R. K., Zon, L. I. and Layton, J. E. (2002). Zebrafish SPI-1 (PU.1) marks a site of myeloid development independent of primitive erythropoiesis: implications for axial patterning. *Dev. Biol.* **246**, 274-295.
Lyons, I., Parsons, L. M., Hartley, L., Li, R., Andrews, J. E., Robb, L. and Harvey, R. P. (1995). Myogenic and morphogenetic defects in the heart tubes of murine embryos lacking the homeo box gene *Nkx2-5*. *Genes Dev.* **9**, 1654-1666.
Meyer, D. and Birchmeier, C. (1995). Multiple essential functions of neuregulin in development. *Nature* **378**, 386-390.
Moorman, A. F. and Christoffels, V. M. (2003). Cardiac chamber formation: development, genes, and evolution. *Physiol. Rev.* **83**, 1223-1267.
Myers, D. C., Sepich, D. S. and Solnica-Krezel, L. (2002). Bmp activity gradient regulates convergent extension during zebrafish gastrulation. *Dev. Biol.* **243**, 81-98.
O'Brien, T. X., Lee, K. J. and Chien, K. R. (1993). Positional specification of ventricular myosin light chain 2 expression in the primitive murine heart tube. *Proc. Natl. Acad. Sci. USA* **90**, 5157-5161.
Rebagliati, M. R., Toyama, R., Fricke, C., Haffter, P. and Dawid, I. B. (1998a). Zebrafish nodal-related genes are implicated in axial patterning and establishing left-right asymmetry. *Dev. Biol.* **199**, 261-272.
Rebagliati, M. R., Toyama, R., Haffter, P. and Dawid, I. B. (1998b). *cyclops* encodes a nodal-related factor involved in midline signaling. *Proc. Natl. Acad. Sci. USA* **95**, 9932-9937.
Redkar, A., Montgomery, M. and Litvin, J. (2001). Fate map of early avian cardiac progenitor cells. *Development* **128**, 2269-2279.
Reiter, J. F., Verkade, H. and Stainier, D. Y. (2001). Bmp2b and Oep promote early myocardial differentiation through their regulation of *gata5*. *Dev. Biol.* **234**, 330-338.
Rosenquist, G. C. (1966). A radioautographic study of labeled grafts in the chick blastoderm. Development from primitive-streak stages to stage 12. *Carnegie Contrib. Embryol.* **262**, 31-110.
Rosenquist, G. C. (1970). Location and movements of cardiogenic cells in the chick embryo: the heart-forming portion of the primitive streak. *Dev. Biol.* **22**, 461-475.
Sampath, K., Rubinstein, A. L., Cheng, A. M., Liang, J. O., Fekany, K., Solnica-Krezel, L., Korzh, V., Halpern, M. E. and Wright, C. V. (1998). Induction of the zebrafish ventral brain and floorplate requires cyclops/nodal signalling. *Nature* **395**, 185-189.
Sato, M. and Yost, H. J. (2003). Cardiac neural crest contributes to cardiomyogenesis in zebrafish. *Dev. Biol.* **257**, 127-139.
Schier, A. F. (2001). Axis formation and patterning in zebrafish. *Curr. Opin. Genet. Dev.* **11**, 393-404.
Sepich, D. S., Myers, D. C., Short, R., Topczewski, J., Marlow, F. and Solnica-Krezel, L. (2000). Role of the zebrafish *trilobite* locus in gastrulation movements of convergence and extension. *Genesis* **27**, 159-173.
Stainier, D. Y. R., Lee, R. K. and Fishman, M. C. (1993). Cardiovascular development in the zebrafish. I. Myocardial fate map and heart tube formation. *Development* **119**, 31-40.
Stalsberg, H. and DeHaan, R. L. (1969). The precardiac areas and formation of the tubular heart in the chick embryo. *Dev. Biol.* **19**, 128-159.
Thisse, C. and Thisse, B. (1999). Antivin, a novel and divergent member of the TGFβ superfamily, negatively regulates mesoderm induction. *Development* **126**, 229-240.
Warga, R. M. and Kimmel, C. B. (1990). Cell movements during epiboly and gastrulation in zebrafish. *Development* **108**, 569-580.
Warga, R. M. and Nüsslein-Volhard, C. (1999). Origin and development of the zebrafish endoderm. *Development* **126**, 827-838.
Woo, K., Shih, J. and Fraser, S. E. (1995). Fate maps of the zebrafish embryo. *Curr. Opin. Genet. Dev.* **5**, 439-443.
Yelon, D. (2001). Cardiac patterning and morphogenesis in zebrafish. *Dev. Dyn.* **222**, 552-563.
Yelon, D., Horne, S. A. and Stainier, D. Y. (1999). Restricted expression of cardiac myosin genes reveals regulated aspects of heart tube assembly in zebrafish. *Dev. Biol.* **214**, 23-37.
Yelon, D. and Stainier, D. Y. (1999). Patterning during organogenesis: genetic analysis of cardiac chamber formation. *Semin. Cell Dev. Biol.* **10**, 93-98.
Yutzey, K. E., Rhee, J. T. and Bader, D. (1994). Expression of the atrial-specific myosin heavy chain AMHC1 and the establishment of anteroposterior polarity in the developing chicken heart. *Development* **120**, 871-883.